Authors accepted manuscript

Di Mare, M., & Ouellet-Plamondon, C. (2022). The effect of composition on the dielectric properties of alkali activated materials: A next generation dielectric ceramic. *Materials Today Communications*, *32*, 104087. https://doi.org/10.1016/j.mtcomm.2022.104087

Title

The effect of composition on the dielectric properties of alkali activated materials: a next generation dielectric ceramic

Authors

Michael Di Mare[1] and Claudiane Ouellet-Plamondon[1]*

[1]: Department of Construction Engineering, University of Quebec, École de technologie supérieure, Montréal, QC, H3C 1K3, Canada.

* Corresponding author: Claudiane.Ouellet-Plamondon@etsmtl.ca

Keywords:

Dielectric constant, linear dielectric, energy storage, alkali activated material, inorganic polymer

Abstract

Alkali activated materials have been modified to achieve dielectric constants over 10^9: the highest dielectric constants ever reported for a ceramic-like material. This is a one-million-fold improvement over barium titanate and strontium titanate dielectric ceramics. It is four orders of magnitude greater than calcium copper titanate: the highest performing dielectric ceramic. Alkali activated materials are a sustainable ceramic-like material, synthesized from byproduct fly ash without the need for calcination or sintering. This exceptional dielectric constant has not been previously reported due to the strong dependence on the elemental composition and activator type. A multivariable compositional optimization was conducted with broadband dielectric spectroscopy to maximize the dielectric performance. With this alkali activated material, the next generation of ceramic capacitors will dramatically improve in affordability, sustainability, and energy storage capacity.

1 Introduction

The transition to intermittent renewable energy sources, such as solar and wind power, creates a demand for high-capacity energy storage systems that are low-cost to install and maintain. Energy storage technology is divided into dielectric capacitors, electrochemical capacitors, and batteries; each with different ranges of specific energy density and power density capabilities. Dielectric capacitors are ubiquitous, versatile, and competitive in cost but limited in their energy storage capacity [1]. For decades, researchers have sought to improve the energy storage capacity by developing new dielectric materials with higher dielectric constants. To date, the greatest dielectric constants have been achieved with calcium copper titanate and barium strontium titanate which can, under precise compositional and fabrication specifications, reach dielectric constants above 10^5 [2,3]. In this work, a facile method is described to produce a novel dielectric material at a bulk scale which surpasses the most refined dielectric ceramics and achieves dielectric constants above 10^9. This could improve the energy storage capacity of dielectric capacitors by a factor of one thousand and revolutionize static energy storage systems.

Improved dielectric constants translate to an enhanced energy storage capacity. The energy stored in a dielectric capacitor is proportional to dielectric constant. Great increases in dielectric constant have been found in conventional dielectric ceramics, e.g. barium titanate, by carefully controlling the elemental composition of the ceramic [1]. Refinement of the composition is responsible for improvement in barium titanate dielectric constants from around 100 to above 10^3 [4,5]. However, this methodology of compositional control has not been applied to all dielectric materials. Alkali activated materials (AAM) are a class of ceramic-like glasses that are known to exhibit high dielectric constants but have been generally overlooked as dielectric materials due to their cement-like mechanical and setting properties [6]. In this study, a four-factor compositional optimization

was conducted in a factorial experimental design to maximize the dielectric constant of AAM. The results exceeded expectations and yielded a dielectric AAM with polarizability far exceeding that of dielectric ceramics.

Dielectric ceramics are categorized as linear dielectrics, ferroelectrics, relaxor ferroelectrics, or antiferroelectrics based the hysteresis in their polarization. The hysteresis arises from remnant polarization during charging and discharging which leads to nonrecoverable energy loss [7]. The majority of research attention has been focused on ferroelectrics (e.g. barium titanate) and antiferroelectrics (e.g. perovskite ceramics) because of the high dielectric constants of these materials. In contrast, linear dielectrics exhibit no hysteresis in their polarization resulting in greater energy recovery [7]. This behavior occurs in centrosymmetric crystals, such as aluminum oxide, and glasses. Linear dielectrics have desirable high breakdown voltages, but their application is limited by their lower saturated polarization due to relatively low dielectric constants [1]. Few studies have overcome this obstacle by discovering new centrosymmetric or amorphous materials with linear dielectric behavior and high dielectric constants.

The search for new linear dielectric requires the recognition of novel materials. Research in dielectric ceramics is predominantly focused on incremental improvements in the elemental optimization of perovskite ceramics [7,8]. These studies do not address the fundamental challenges in scalability and cost which limit the deployment of high performing dielectric ceramics in energy storage infrastructure. Prior studies that have proposed creative material solutions to address these challenges, such as cement-based supercapacitors [9,10], have received little attention from the electronic ceramics community. Thus, it has been without fanfare that the dielectric constants of AAM have been reported to be above 10^4 [6,11], despite this property exceeding the performance of ferroelectric ceramics. AAM are construction-grade materials, boasting low cost, high

production volumes, and low environmental impact [12]. Their use as an alternative dielectric addresses a fundamental challenge in the production of affordable energy storage systems.

The lack of understanding of the dielectric behavior of AAM has led neglect of their potential. Unlike dielectric ceramics which are stable over large ranges of frequency, the dielectric polarization in AAM is understood to arise, not from dipoles, but from interfacial polarization. As such, the large dielectric constant of AAM has been interpreted as a consequence of ionic mobility of super-stoichiometric alkali cations within the amorphous structure [13]. This causes AAM to have relatively high loss tangents and strong frequency dependence in their permittivity [6,14]. The composition of the AAM plays a large role in the dielectric behavior [11,14]. AAM are amorphous aluminosilicate materials with complex chemistry, defined by an elemental proportion (alkali:aluminum:silicon ratio), the type of alkali ion, and the type of activator [15]. Preliminary studies have shown for sodium AAM that increasing the alkali content (Na/Al ratio) can increase the dielectric constant to nearly 10^5 and that switching from sodium to potassium can offer further enhancement [14,16]. However, the scientific literature on the dielectric properties of AAM is thin and effect of other the compositional parameters is entirely unknown.

This study addresses this gap in the literature explore the synergy between different compositional factors and maximize the dielectric constant of AAM. A four-factor optimization was conducted to determine the effect of alkali content (K/Al ratio), monomer structure (Si/Al ratio), activator anions, and testing frequency on the dielectric constant, loss tangent, and ionic conductivity. The permittivity is known to be sensitive to frequency and the results will seek to support the hypothesis that this relationship is connected to the ionic conductivity. The effect of the alkali content is known for sodium AAM but has not been studied in potassium AAM. The monomer structure is determined by the ratio of silica and alumina tetrahedra and is known to have a large impact on

the mechanical strength and density but has never been previously considered in the study of the dielectric properties of AAM [17]. Finally, the activator anion influences the mechanical strength, setting time, and environmental impact of AAM, but the effect of their chemistry on the dielectric polarization has not been studied [18–20]. These four factors were studied with a factorial experimental design to elucidate the synergies between each factor. This analysis comprehensively establishes the optimal composition of potassium AAM to maximize the dielectric constant.

2 Experimental procedures

To measure the dielectric properties, specimens of alkali activated material (AAM) were prepared by the alkali activation of fly ash (ProAsh®, Separation Technologies LLC). The fly ash was composed of 55.3% silicon oxide, 21.4% aluminum oxide, 10.2% iron oxide, 3.4% calcium oxide, and 2.1% potassium oxide. The silicon:aluminum ratio of the AAM was modified by the addition of silica fume to the fly ash. The silica fume was deagglomerated in a pulverizing pan prior to addition to ensure dispersion and measured to have a moisture content of 4.8%. Two reagent grade potassium salts were tested separately as activators: potassium hydroxide (12% moisture) and potassium carbonate (0.1% moisture). Specimens were prepared in arrays of potassium:aluminum (K/Al) and silicon:aluminum (Si/Al) ratios with each activator, centered around the composition 1:1:2.85 (K/Al/Si). This composition was previously reported to exhibit a high dielectric constant [16]. The water content was kept constant at a liquid to solids ratio of 0.18 to ensure flowable AAM pastes across the compositional range.

Table 1: Composition of experimental specimens.

Sample ID	Activator anion	K / Al ratio	Si / Al ratio	Fly ash (g)	Silica fume (g)	Activator (g)	Water (g)
H-0.8-2.5	Hydroxide	0.8	2.5	100	7.8	18.6	17.6
H-1-2.5	Hydroxide	1.0	2.5	100	7.8	25.0	17.7
H-1.2-2.5	Hydroxide	1.2	2.5	100	7.8	29.3	17.8
H-1.4-2.5	Hydroxide	1.4	2.5	100	7.8	34.6	17.9
H-0.8-2.85	Hydroxide	0.8	2.85	100	15.8	18.6	18.9
H-1-2.85	Hydroxide	1.0	2.85	100	15.8	25.0	19.0
H-1.2-2.85	Hydroxide	1.2	2.85	100	15.8	29.3	19.0
H-1.4-2.85	Hydroxide	1.4	2.85	100	15.8	34.6	19.1
H-1-2.3	Hydroxide	1.0	2.3	100	3.6	25.0	17.0
H-1-2.7	Hydroxide	1.0	2.7	100	12.1	25.0	18.4
H-1-3	Hydroxide	1.0	3.0	100	20.5	25.0	19.7
H-1-3.2	Hydroxide	1.0	3.2	100	24.7	25.0	20.4
H-1.4-2.3	Hydroxide	1.4	2.3	100	3.6	34.6	17.2
H-1.4-2.7	Hydroxide	1.4	2.7	100	12.1	34.6	18.5
H-1.4-3	Hydroxide	1.4	3.0	100	20.5	34.6	19.9
C-0.8-2.5	Carbonate	0.8	2.5	100	7.8	18.9	24.1
C-1-2.85	Carbonate	1.0	2.85	100	15.8	27.0	25.6
C-1.2-2.85	Carbonate	1.2	2.85	100	15.8	31.6	26.4
C-1.4-2.85	Carbonate	1.4	2.85	100	15.8	37.7	27.5
C-1.6-2.85	Carbonate	1.6	3.0	100	15.8	43.2	28.5
C-1.8-2.85	Carbonate	1.8	3.0	100	15.8	49.0	29.5
C-2-2.85	Carbonate	2.0	3.0	100	15.8	56.5	30.9
C-1-2.3	Carbonate	1.0	2.3	100	3.6	27.0	23.4
C-1-2.5	Carbonate	1.0	2.5	100	7.8	27.0	24.2
C-1-2.7	Carbonate	1.0	2.7	100	12.1	27.0	24.9
C-1-3	Carbonate	1.0	3.0	100	20.5	27.0	26.4
C-1-3.2	Carbonate	1.0	3.2	100	24.7	27.0	27.2
C-1.4-2.3	Carbonate	1.4	2.3	100	3.6	37.7	25.3
C-1.4-2.5	Carbonate	1.4	2.5	100	7.8	37.7	26.1
C-1.4-2.7	Carbonate	1.4	2.7	100	12.1	37.7	26.8
C-1.4-3	Carbonate	1.4	3.0	100	20.5	37.7	28.3
C-1.4-3.2	Carbonate	1.4	3.2	100	24.7	37.7	29.1

The mixing of the AAM paste was conducted in a low shear mixer with a radial flow impeller. The AAM were prepared with a one-part mixing methodology to enhance the scalability of the

process. The powders, fly ash, silica fume, and activator, were gently premixed by hand until a homogenous powder was obtained which achieves the desired elemental ratio (K/Al/Si). Then, deionized water was added to achieve the targeted liquid to solid ratio. The mixture was mixed for five minutes at 200 rpm until a homogenous paste was obtained. The paste was immediately cast into polyoxymethylene molds. Disks of diameter 40 mm and thickness 2 mm were prepared for broadband dielectric spectroscopy, as shown in Figure 1(d). The samples of each composition were cured at 60ºC for two days in a sealed environment to prevent moisture loss. Subsequently, they were dried at 60ºC for one day to remove surface moisture without decomposing the native hydrates in the AAM.

In the performance of a dielectric, two material properties must be considered: the dielectric constant and the loss tangent. The dielectric constant is directly proportional to the energy storage capacity of a capacitor. The loss tangent quantifies the amount of energy that is lost to heat during charging. The dielectric properties and conductivity of the specimens were measured by broadband dielectric spectroscopy (Novocontrol Technologies GmbH) at room temperature. A quadratic profile wave of amplitude three volts was applied cyclically at room temperature at frequencies between 0.1 Hz and 1 MHz. Specimens were prepared in quadruplicate and averaged to produce the results shown. Additional specimens were prepared for cyclic voltammetry. The pastes were mixed in an identical manner and cast into 5 cm cubes. A mounted bracket was used to maintain a pair of stainless-steel mesh electrodes in parallel at a spacing of 1 cm apart. The specimens were cured in a sealed environment, to prevent moisture loss, and then dried in the same manner described above. Cyclic voltammetry was conducted using a source measurement unit (2450 SourceMeter, Keithley Instruments), a voltage of $\pm$1 Volts, and a scan speed of 1 Hz.

3 Results and discussion

3.1 Dielectric properties of potassium hydroxide activated fly ash

Broadband dielectric spectroscopy analyzes the frequency dependence of the electrical and dielectric properties of a material. The dielectric behavior of alkali activated materials (AAM) is known to vary significantly with frequency [11]. The frequency dependence of the dielectric constant, loss tangent, and conductivity for four AAM is shown in Figure 1. The relationships agree with previously reported trends for AAM [6,14]. The dielectric constant, Figure 1(a), exhibits two slopes: a nearly constant dielectric constant above 10 kHz and a constant exponential increase at lower frequencies. Above 100 kHz, the dominant polarization mechanism is dipolar, caused by local shifts in the ions within the amorphous AAM structure. This is corroborated by the two-regime conductivity shown in Figure 1(c). At high frequencies, the conductivity is predominantly electrical, while at low frequencies the conductivity approaches a lower, constant value indicating that it is caused by mobility of alkali ions, particularly potassium, which are loosely bound to alumina tetrahedra in the AAM structure [15]. Greater ionic conduction at low frequency drives ionic-interfacial polarization, which is responsible for the high dielectric constants reached at low frequency. This polarization is caused by the electrostatic accumulation of ions along interfaces and grain boundaries within the AAM, due to ionic conduction in the presence of the external electric field [21]. The contribution of this polarization is enhanced at low frequencies because the greater period gives more ions time to migrate to the interfaces, increasing the total polarization.

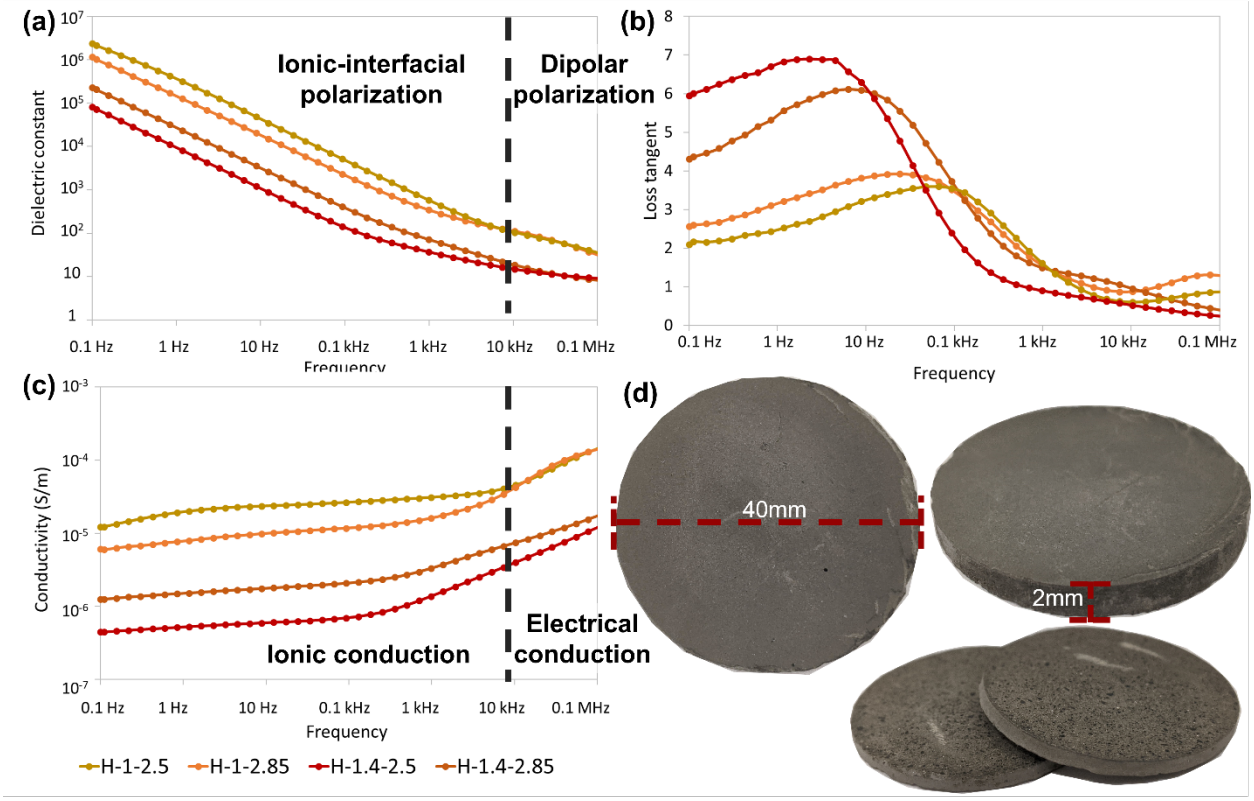

Figure 1: Broadband dielectric spectroscopy of potassium hydroxide AAM with different elemental compositions, defined by the K/Al/Si ratio, for (a) dielectric constant, (b) loss tangent, and (c) conductivity. (d) AAM experimental specimen prepared for analysis.

The impedance to polarization is known as dielectric relaxation and is summarized by the loss tangent, shown in Figure 1(b). Dielectric relaxation is a material property influenced by its structure. The changing frequency positions of the peaks in loss tangent are an indication of structural differences between the amorphous AAM and the influence of the elemental proportion on the structure [22]. The shift in the loss tangent peaks confirms the impact of the elemental proportions of the AAM on the dielectric properties, which can also be seen in the dielectric constant and conductivity. The four AAM shown in Figure 1 form two pairs based on their potassium:aluminum (K/Al) ratio, indicating that this factor has a significant influence on the dielectric properties and conductivity. This trend agrees with previous reports of the effect of alkali

content in sodium-based AAM [14]. However, the silicon:aluminum (Si/Al) ratio, which has not been considered in any previous study, can also be seen to have a substantial impact on both the dielectric constant and the conductivity.

Table 2: Summary of dielectric properties of potassium hydroxide activated inorganic polymers based on their elemental ratio.

Sample ID	K / Al ratio	Si / Al ratio	Dielectric constant at 0.1 Hz	Dielectric constant at 50-60 Hz	Conductivity at 50-60 Hz (S/m)
H-0.8-2.5	0.8	2.5	5.0×10^{3}	1.2×10^{2}	3.0×10^{-9}
H-1-2.5	1.0	2.5	1.5×10^{6}	1.0×10^{3}	1.6×10^{7}
H-1.2-2.5	1.2	2.5	7.2×10^{3}	8.0×10^{1}	3.1×10^{-9}
H-1.4-2.5	1.4	2.5	1.2×10^{4}	7.1×10^{1}	5.2×10^{-9}
H-0.8-2.85	0.8	2.85	3.7×10^{3}	1.1×10^{2}	2.4×10^{-9}
H-1-2.85	1.0	2.85	5.5×10^{5}	9.7×10^{2}	1.5×10^{-7}
H-1.2-2.85	1.2	2.85	7.4×10^{4}	2.3×10^{2}	2.2×10^{-8}
H-1.4-2.85	1.4	2.85	4.3×10^{4}	1.2×10^{2}	1.7×10^{-8}
H-1-2.3	1.0	2.3	5.5×10^{3}	6.2×10^{1}	2.8×10^{-9}
H-1-2.7	1.0	2.7	1.7×10^{5}	3.7×10^{2}	4.8×10^{-8}
H-1-3	1.0	3.0	8.0×10^{3}	1.2×10^{2}	5.2×10^{-9}
H-1-3.2	1.0	3.2	4.5×10^{3}	8.5×10^{1}	2.9×10^{-9}
H-1.4-2.3	1.4	2.3	2.1×10^{5}	3.0×10^{2}	4.6×10^{-8}
H-1.4-2.7	1.4	2.7	6.1×10^{3}	5.6×10^{1}	3.2×10^{-9}
H-1.4-3	1.4	3.0	2.6×10^{3}	4.0×10^{1}	1.8×10^{-9}

To further the effect of these two elemental ratios on these two properties, an array of compositions was tested with varying combinations of K/Al and Si/Al ratios. The dielectric constant and conductivity in the 50-60 Hz range, which is of principle interest in conventional energy storage, is given in Table 2. The dielectric properties were found to be strongly dependent on the elemental ratios. There is a strong correlation between the compositions which exhibited higher dielectric constant with greater conductivity. This further supports the hypothesis proposed by other works that the large dielectric polarization of AAM is caused by ionic conductivity and ionic-interfacial

polarization [13]. The composition H-1-2.5 exhibited the highest dielectric constant, 10^3 at 50-60 Hz. This is comparable to barium titanate at the same frequency [4,5,8]. However, unlike barium titanate and other ferroelectric ceramics, the dielectric constant is dramatically increased at low frequency. The dielectric constant, shown in Figure 1(a), exponentially increases at lower frequencies and can reach exceedingly high values at pseudo-direct current conditions, such as 0.1 Hz. At 0.1 Hz, the H-1-2.5 composition reaches a dielectric constant of 10^6, which is 1000 times higher than barium titanate and 200 times higher than barium strontium titanates [4,8,23–25]. The increased dielectric constant at low frequencies occurs in all compositions, as shown in Table 2, and is enhanced for compositions which are more favorable to polarization at 50-60 Hz.

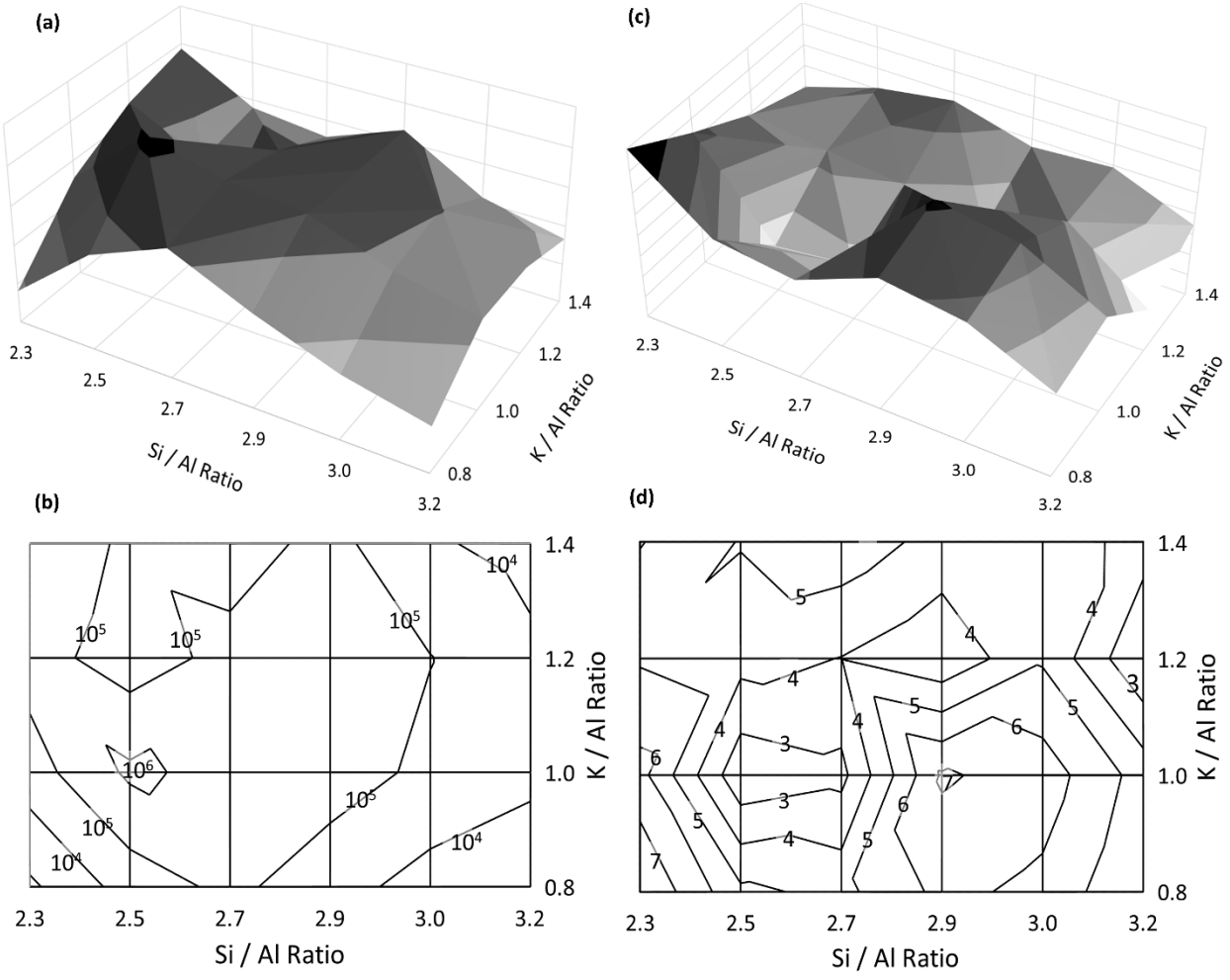

Figure 2: (a,b) The compositional dependence of the dielectric constant at 0.1 Hz visualized as (a) a 3D rendering and (b) a contour plot. (c,d) The loss tangent at 0.1 Hz illustrated with (c) a 3D rendering and (d) a contour plot across the compositional array

To map the effect of the elemental ratios on the dielectric constant and understand the effect of the AAM structure on the dielectric properties, the dielectric properties at 0.1 Hz were visualized in the manner shown in Figure 2. The effect of the K/Al and Si/Al ratios are not independent, as shown in the 3D rendering and contour plot of Figure 2(a,b), with a maximum that is interdependent on both factors. Prior literature on the topic has solely considered the impact of alkali content (K/Al) on the dielectric constant [14,26]. However, Figure 2(b) clearly shows that both the alkali content and the monomer structure (Si/Al) are equally important. In the range of Si/Al ratio 2.0 to 3.0, AAM are understood to be composed of a mixture of sialate-siloxo and silate-disiloxo monomers [15]. For potassium hydroxide AAM, the maximum was observed at a Si/Al ratio 2.5, indicating that dielectric polarization is maximized when an even distribution of the two types of monomers is present within the AAM. For the optimum composition, H-1-2.5, the 10^6 dielectric constant measured surpasses the highest dielectric constant reported for sodium AAM by a factor of one hundred [14].

There is a correlation between the compositional dependence of the dielectric constant and the loss tangent. The highest dielectric constant and lowest loss tangent are found at the same composition. This is a desirable combination of energy storage applications that seek to store large energy densities while minimizing charging losses. However, dielectric relaxation is mechanistically distinct from the linear polarization which is responsible for the large dielectric constants in AAM. The loss tangent, shown in Figure 2(c,d), does not share precisely the same compositional dependence as the dielectric constant. Moreover, the loss tangent for the potassium hydroxide

AAM, even at the optimized composition of H-1-2.5, is significantly higher than is desired for the application of a linear dielectric. While post-treatment methodologies, such as calcination [27], may be capable at reducing the loss tangent, they add cost and processing complexity which reduces one of the key advantages of AAM over conventional dielectric ceramics. A more desirable solution is the discovery of a better AAM composition which further improves the dielectric properties.

3.2 Maximizing the dielectric constant with potassium carbonate activated fly ash

In search of alkali activated materials (AAM) with high dielectric constant and low loss tangent, an alternative potassium activator was investigated. An array of potassium carbonate AAM were prepared with varying K/Al and Si/Al ratios and analyzed by broadband dielectric spectroscopy. The dielectric properties and conductivity exhibited equivalent frequency dependence to potassium hydroxide AAM discussed previously. However, the dielectric constant and conductivity were significantly higher than the AAM activated with potassium hydroxide, as shown in Table 3. At 50-60 Hz, the dielectric constant exceeds 10^6 for some compositions and at the optimum composition, C-1.4-2.85, the dielectric constant reaches 10^9 at 0.1 Hz, a 1000-fold increase over that of the potassium hydroxide AAM. This is the highest dielectric constant ever reported for a ceramic-like dielectric.

Table 3: Summary of the dielectric properties of potassium carbonate activated inorganic polymers based on their elemental ratio.

Sample ID	K / Al ratio	Si / Al ratio	Dielectric constant at 0.1 Hz	Dielectric constant at 50-60 Hz	Conductivity at 50-60 Hz (S/m)
C-0.8-2.5	0.8	2.5	8.8×10^6	2.3×10^4	2.5×10^{-4}

C-1-2.85	1.0	2.85	5.7×10^{6}	7.5×10^{3}	9.9×10^{-5}
C-1.2-2.85	1.2	2.85	6.7×10^{8}	4.2×10^{6}	3.8×10^{-2}
C-1.4-2.85	1.4	2.85	1.1×10^{9}	3.5×10^{6}	2.1×10^{-2}
C-1.6-2.85	1.6	3.0	2.0×10^{8}	2.5×10^{5}	3.2×10^{-3}
C-1.8-2.85	1.8	3.0	2.2×10^{8}	3.5×10^{5}	6.5×10^{-3}
C-2-2.85	2.0	3.0	1.0×10^{8}	2.1×10^{5}	3.1×10^{-3}
C-1-2.3	1.0	2.3	8.0×10^{7}	3.4×10^{5}	3.9×10^{-3}
C-1-2.5	1.0	2.5	2.7×10^{7}	3.8×10^{4}	7.3×10^{-4}
C-1-2.7	1.0	2.7	1.2×10^{6}	2.4×10^{3}	3.6×10^{-5}
C-1-3	1.0	3.0	1.7×10^{5}	3.1×10^{2}	4.3×10^{-6}
C-1-3.2	1.0	3.2	1.5×10^{2}	4.8×10^{1}	6.6×10^{-8}
C-1.4-2.3	1.4	2.3	8.1×10^{7}	1.8×10^{5}	2.1×10^{-3}
C-1.4-2.5	1.4	2.5	8.1×10^{6}	5.6×10^{4}	5.9×10^{-4}
C-1.4-2.7	1.4	2.7	7.8×10^{6}	1.1×10^{4}	1.7×10^{-4}
C-1.4-3	1.4	3.0	2.5×10^{7}	4.3×10^{4}	7.8×10^{-4}
C-1.4-3.2	1.4	3.2	1.3×10^{7}	1.9×10^{4}	3.1×10^{-4}

Comparing the results of Table 2 and Table 3 based on the elemental ratios reveals that the activator anion has a large impact on the polarizability of the AAM. The effect of activator anion has never been previously investigated or reported for electrical or dielectric properties. The results also indicate that the optimal elemental ratios, which give the highest dielectric constant, are different for different activators. To elucidate the changing compositional relationships, the dielectric properties of the potassium carbonate AAM were visualized in Figure 3 in a manner to mimic Figure 2. For this activator, the optimum K/Al ratio is shifted to 1.4, indicating that a supersaturation of potassium ions enhances the ionic conduction which is responsible for the ionic-interfacial polarization. As was found with the potassium hydroxide AAM, the loss tangent and dielectric constant are inversely related, which is a desirable for dielectric applications, and the loss tangent is reduced to 1.3. The exceptionally high dielectric constant of potassium carbonate AAM warrants additional investigation to leverage this property.

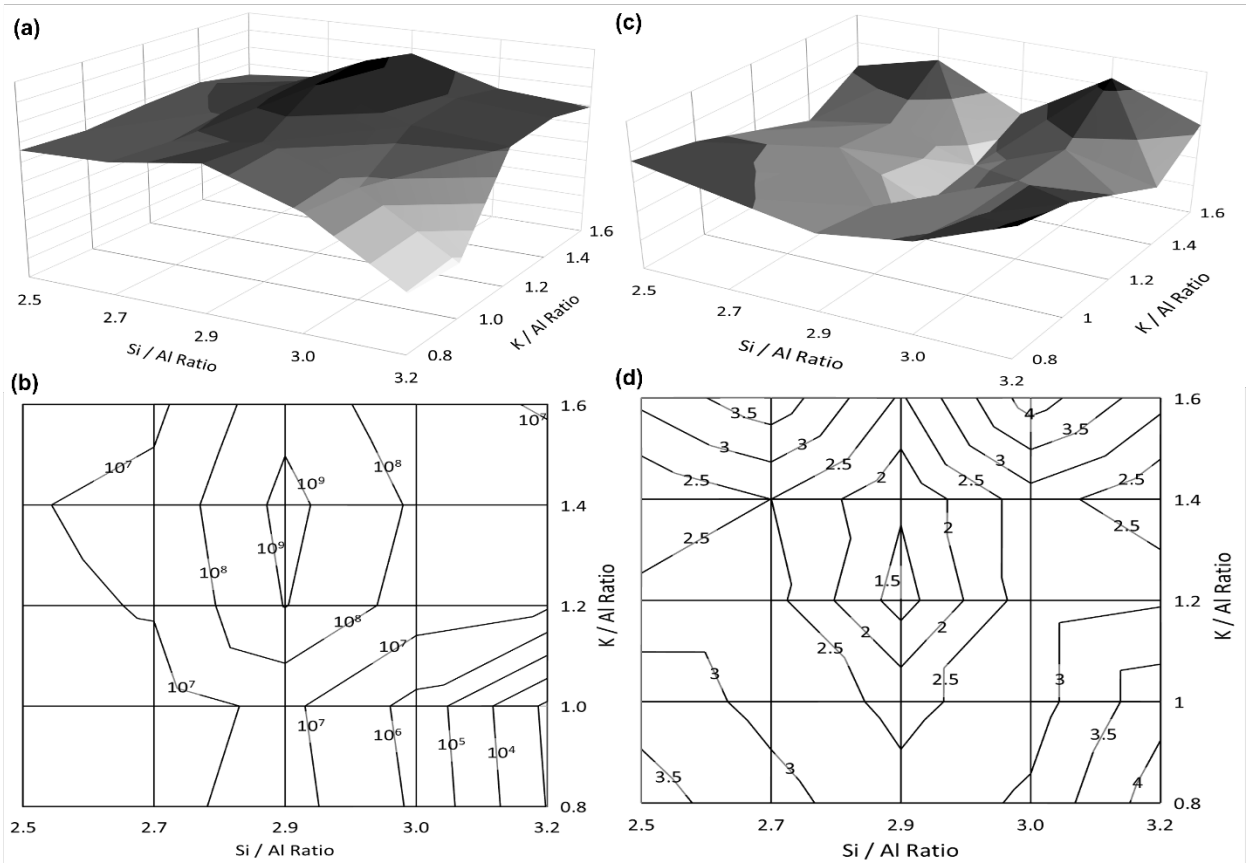

Figure 3: (a,b) The dielectric constant of potassium carbonate AAM at 0.1 Hz visualized in (a) a 3D rendering and (b) a contour plot. (c,d) The loss tangent at 0.1 Hz illustrated with (c) a 3D rendering and (d) a contour plot across the compositional array.

With the optimal composition, potassium carbonate AAM exhibit the greatest dielectric constant ever reported in the literature of ceramic dielectrics. To date, calcium copper titanates have been extensively investigated since their discovery in 1967 and are regarded as the highest polarizing dielectric material [28,29]. This ceramic can have a dielectric constant as high as $5x10^4$ at room temperature and low frequency (50 Hz) [3]. Only a few precisely doped ceramic composites have been documented to surpass this record and reach dielectric constants of 10^5 [2,30]. Potassium carbonate AAM offers an unprecedented leap in dielectric constant. This could increase energy storage capacity of capacitors by as much a million times. Moreover, the AAM are produced

without the need for chemical vapor deposition, hydrothermal crystallization, high temperature sintering, or virgin raw materials. A lack of sustainability in energy storage technology is a recognized concern [31]. Dielectric AAM are a major step towards an energy storage technology for sustainable and circular economy. However, realizing this opportunity will require future studies to develop new fabrication methods and to better understand the dielectric loss in AAM.

3.3 Ionic conductivity and energy storage mechanisms

Despite the improvement offered by the potassium carbonate activator, alkali activated materials (AAM) continue to exhibit high loss tangent. Reducing the loss tangent further will require a deeper understanding to the nature of the polarization and dielectric relaxation in AAM. Addressing these underlying questions will require additional investigation outside of the scope of this work, whose objective is to determine the optimum composition of AAM. The results of this study can create a framework for a future investigation into the dielectric mechanisms of AAM. Prior literature on the topic has concluded that the great dielectric polarization in AAM is a consequence of their high ionic conductivity [13,16]. Alkali ions, in this case potassium, act as a charge-balancing species within the amorphous network of the AAM, localized around the alumina tetrahedra. Ionic conduction occurs through charge hopping mechanisms which allow the cations to move to adjacent sites [13]. For potassium carbonate AAM, enhanced dielectric polarization was observed when the alkali content (K/Al) was greater than 1.0. This implies that an excess of potassium cations contributes to improved ionic conductivity, which enhances the dielectric response. This implies the hypothesis that maximizing the conductivity simultaneously maximizes the dielectric constant.

This hypothesis is supported by measurements of the conductivity across the compositional range of elemental ratios. The conductivity of each AAM specimen was measured and the results, at 0.1 Hz, were visualized in Figure 4 for each activator. Comparing Figure 4(a,b) and Figure 2(a,b) reveals a strong positive correlation between the conductivity and dielectric constant for potassium hydroxide AAM. The maxima and minima occur at the same compositions and the overall curvature is identical. The same is true for potassium carbonate AAM, shown in Figure 4(c,d) and Figure 3(a,b). The results corroborate the theory that the ionic conductivity strongly contributes to the dielectric polarization. The conductivity of the potassium carbonate AAM were found to be significantly higher than for potassium hydroxide AAM, reaching 38 mS/m (380 μS/cm) for composition C-1.2-2.85. Notably, this is only one tenth the value reported for some fast ionic conductors [32]. A future study may consider the possibility of improving upon this to create an affordable and sustainable AAM ionic conductor.

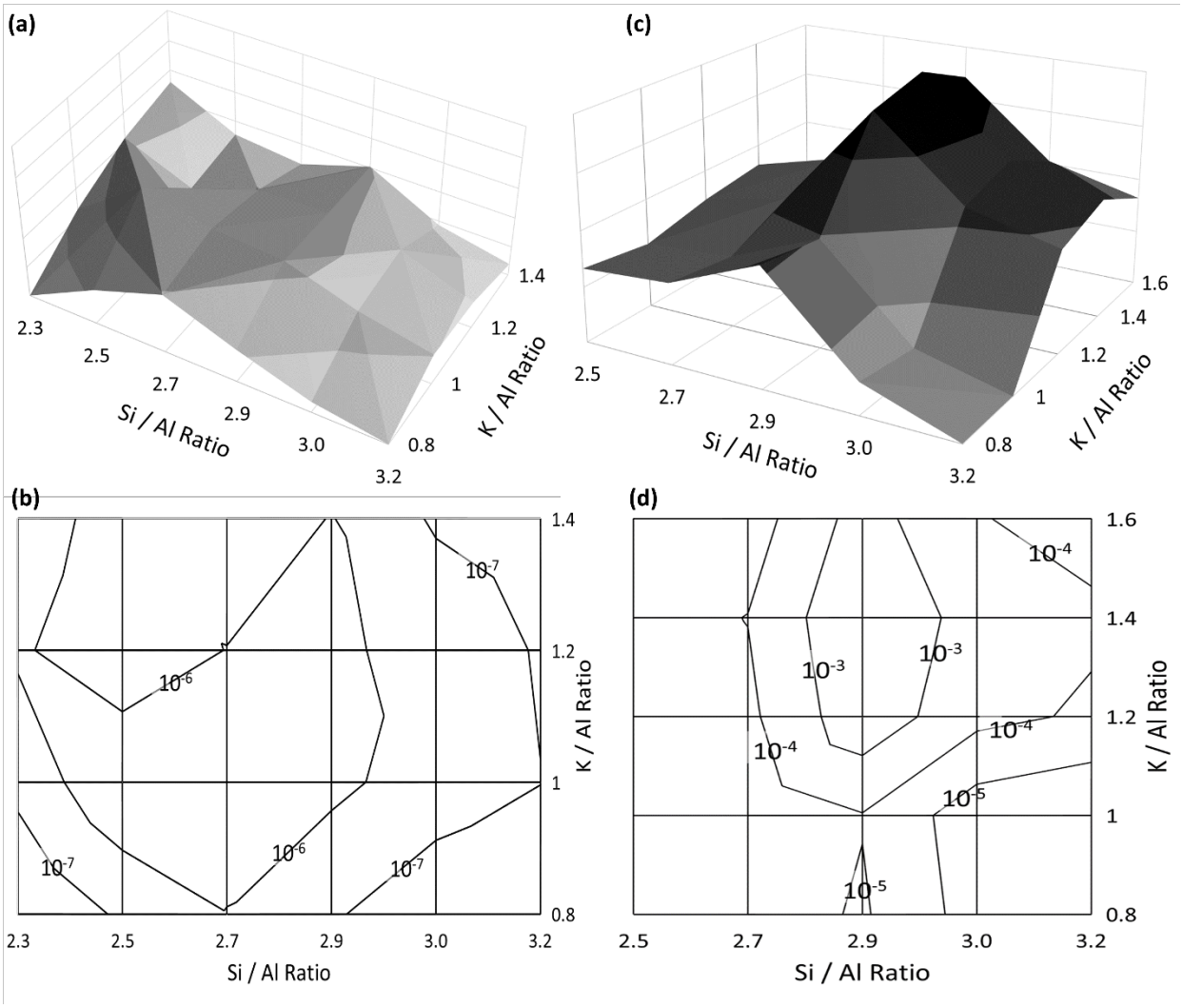

Figure 4: The conductivity (in S/m) of (a,c) potassium hydroxide activated and (b,d) potassium carbonate AAM, illustrated in 3D renderings and contour plots.

Ionic conduction in AAM leads to interfacial polarization and charge accumulation on the electrodes. Prior literature has explained energy storage within AAM through a conduction-adsorption mechanism [16]. Mobile alkali ions accumulate on grain boundaries within the AAM and adsorb on the anode. The ionic accumulation results in the formation of a double layer capacitor on the electrode surfaces, as visualized in Figure 5(d). This mechanism is more kinetically favored at low frequencies, where the ions have more time to move, which explains the

strong frequency dependence of the dielectric polarization. To measure this phenomenon, cyclic voltammetry was conducted on the AAM specimens.

The charge accumulation mechanism which occurs in AAM is fundamentally different than the energy storage mechanism responsible for the behavior of ferroelectric ceramics, such as barium titanate. Unlike barium titanate, AAM are amorphous and cannot have the required space group symmetry for the ferroelectric phenomenon. Thus, energy storge of AAM must be assessed differently than it is done for ferroelectrics. The cyclic voltammetry measurements, shown in Figure 5, offer an alternative measurement to the conventional polarization-electric field (*p*-*E*) analysis used to measure energy storage in ferroelectric and antiferroelectric dielectrics. In this measurement, larger hysteresis represents the formation of a stronger double layer capacitor and a greater total energy storage. The method is employed qualitatively to determine the relative strength of the AAM as an energy storage medium.

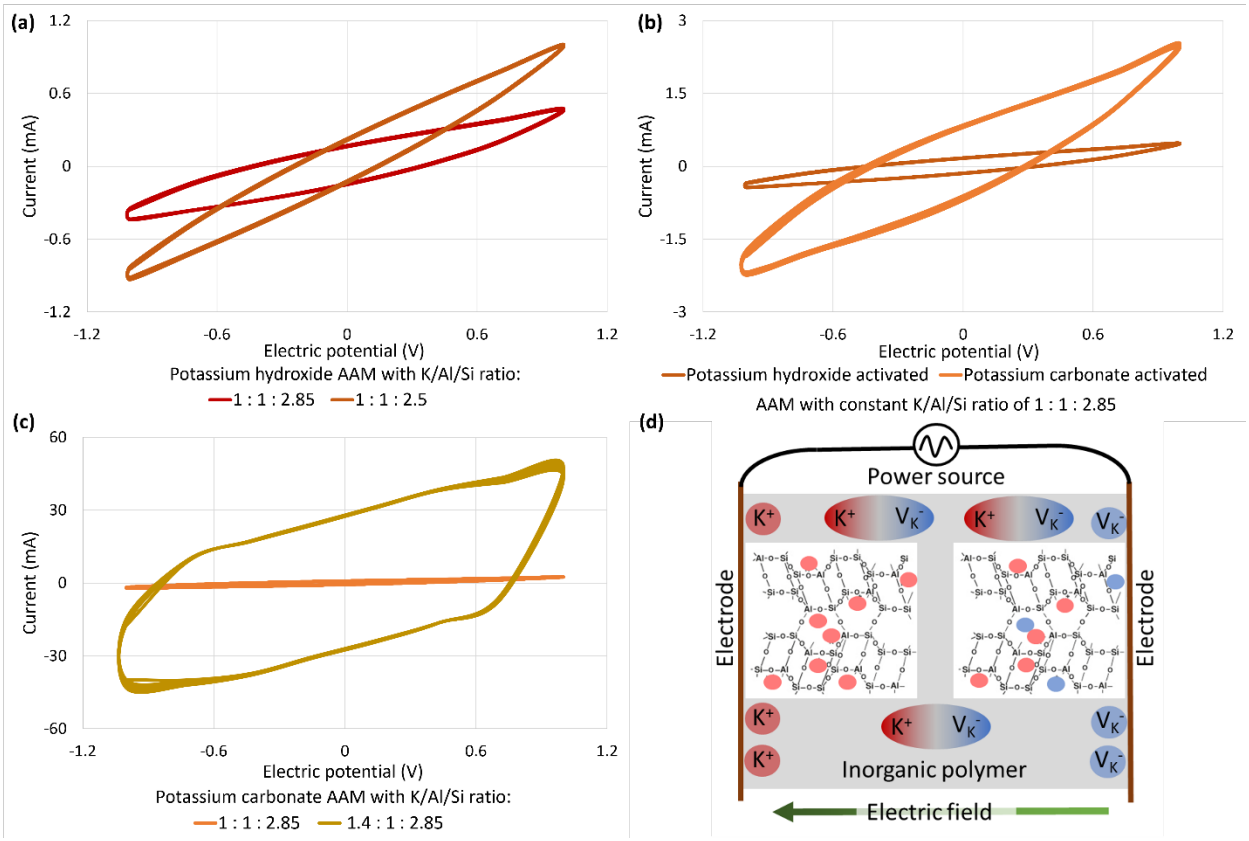

Figure 5: Cyclic voltammetry at 1 Hz of (a) two potassium hydroxide AAM with different elemental compositions, (b) two AAM with different activators but equivalent elemental composition, (c) two potassium carbonate AAM with different elemental compositions. (d) Graphical illustration of dipole formation and ionic conduction to the electrodes. The AAM structure was adapted from *Davidovits 2013,* shared under creative commons CC BY-SA 3.0.

The cyclic voltammetry measurements compare pairs of AAM specimens with different dielectric constants. Figure 5(a) compares two potassium hydroxide AAM specimens: one with dielectric constant 10^5 and the other with 10^6. The difference in voltametric response is relatively low but favors the material with higher dielectric constant. In Figure 5(b), a much larger difference is observed between AAM prepared with different activators which coincides with a larger increase in dielectric constant. This difference is dwarfed by hysteresis of the optimal composition of

potassium carbonate AAM, shown in Figure 5(c). The larger hysteresis indicates a substantially greater accumulation of charges at the electrodes. This supports the hypotheses that ionic conduction and adsorption are occurring in the AAM with higher dielectric constants, resulting in greater energy storage.

3.4 Next steps: continuous casting methods for alkali activated films

Alkali activated materials (AAM) offer a promising solution for high density energy storage in environmentally friendly linear dielectric capacitors. However, their development cannot advance without suitable fabrication methods to produce AAM films. This will enable quantitative measurements of the energy storage capacity and estimates of the production costs compared to conventional alternatives. This topic deserves thorough investigation and is outside the scope of this study. However, due to the importance of this topic as the pivotal next step in the development of AAM dielectrics, a summary of the most suitable fabrication methods has been included here to promote the topic for subsequent study. The ideal methods for producing AAM films must be able to produce comparable thicknesses to that of barium titanate or other dielectric ceramics and support a continuous production to maximize the scalability and affordability of the production. Two methodologies have been identified that meet these ideal requirements, visualized in Figure 6.

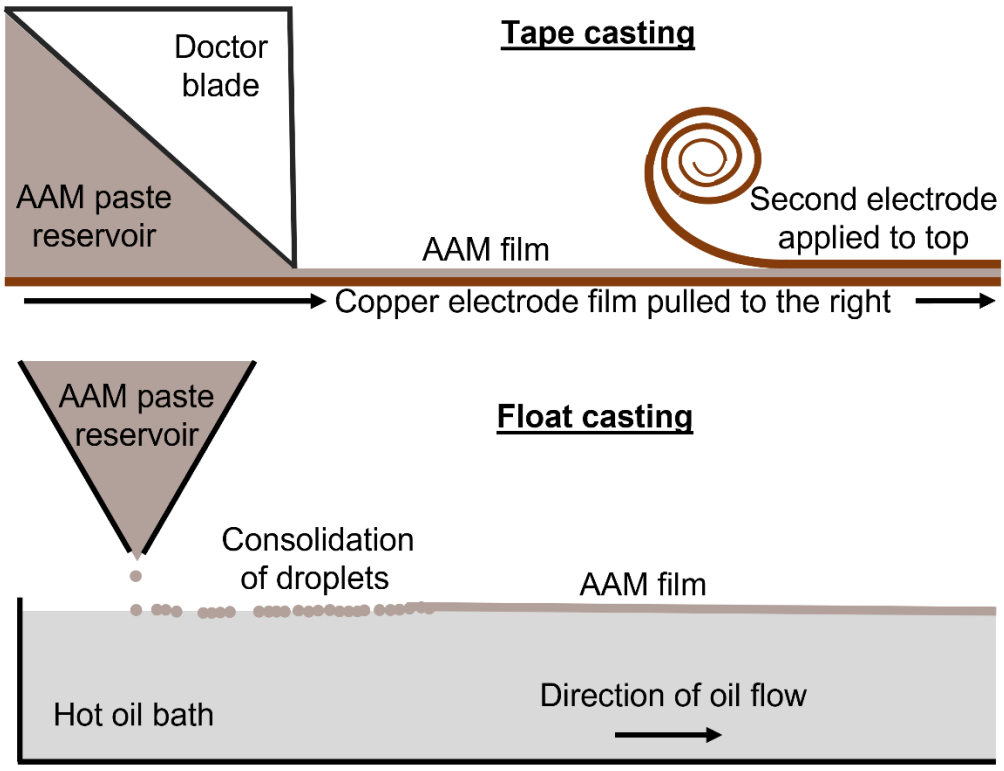

Figure 6: Illustration of tape casting and float casting methods for the continuous fabrication of alkali activated material films.

The two ideal methodologies are tape casting and float casting, conventionally used to produce ceramic greenware and glass lites. Tape casting technique uses a doctor blade and a moving substrate to create continuous films. Tape casting has been demonstrated with AAM for other applications to produce film thicknesses below 100 microns [33,34]. Further refinement of the doctor blade angle, substrate speed, and rheological properties of AAM will be able to reduce this thickness. A similar process refinement has been conducted on barium titanate to produce film thicknesses as low as 3 microns. These films have been deemed suitable for capacitor applications and are advantageous because of the low cost and high throughput of tape casting [35]. In float casting, droplets are cast onto a non-miscible liquid and allowed to consolidate into a film. A similar drip casting method has already been applied to AAM using a hot polyethylene glycol bath

to achieve setting within 30 minutes of casting [36]. Float casting has been successfully implemented for the production of zeolite membranes with film thicknesses as low as 1.7 microns [37,38].

The development of film casting methods for AAM will enable future studies to build AAM capacitors and accurately assess the maximum energy storage capacity. The energy stored in a capacitor is proportional to the dielectric constant and inversely proportional to the thickness. High performing dielectric ceramics are generally synthesized on the scale of 1 micron or, preferably, sub-micron thickness [1]. This this level of thickness may be impossible with tape or float casting, but the million-fold improvement in dielectric constant offered by AAM gives significant room for flexibility in thickness. While conventional dielectric capacitors have energy density below 0.1 Wh/kg, a 10-micron film of potassium carbonate AAM could have an energy density of 10^3 Wh/kg, surpassing the energy density of batteries and that of liquid fuels [1,7]. Moreover, AAM are a low-cost, environmentally friendly alternative to conventional dielectric ceramics that can be prepared from non-virgin raw materials, shaped with continuous production processes, and cured without energy intensive sintering. Combining these advantages with dramatic improvement in energy density is a revolutionary development for energy storage technology.

4 Conclusions

Alkali activated materials (AAM) present a unique opportunity to create high storage dielectric capacitors in a circular economy, recycling industrial wastes into value-added products. AAM are produced from byproduct aluminosilicate wastes and, previously, their dielectric properties have received very little scientific attention. This manuscript describes the methods to produce and

optimize AAM with exceptionally high dielectric constants, up to 10^9. This is the highest dielectric constant ever reported in a ceramic-like material. Future studies must develop new film casting methods to produce homogenous and uniform AAM dielectric capacitors. With tape or float casting methods, low-cost circular economy AAM capacitors could achieve energy storage capacities comparable to conventional batteries. This is more than a thousand-fold improvement over conventional capacitors. AAM dielectric capacitors are an environmentally conscious solution to energy storage and warrant further recognition and investigation.

5 Conflicts of interest

There are no conflicts to declare.

6 Acknowledgements

The authors would like to thank the Natural Sciences and Engineering Research Council of Canada for their support of this research.

7 References

[1] X. Hao, A review on the dielectric materials for high energy-storage application, J. Adv. Dielect. 03 (2013) 1330001. https://doi.org/10.1142/S2010135X13300016.
[2] Y. Zhang, T. Ma, X. Wang, Z. Yuan, Q. Zhang, Two dielectric relaxation mechanisms observed in lanthanum doped barium strontium titanate glass ceramics, Journal of Applied Physics. 109 (2011) 084115.
[3] S. Jesurani, S. Kanagesan, R. Velmurugan, T. Kalaivani, Phase formation and high dielectric constant of calcium copper titanate using sol–gel route, Journal of Materials Science: Materials in Electronics. 23 (2012) 668–674. https://doi.org/10.1007/s10854-011-0468-9.

[4] K. Yao, L. Zhang, X. Yao, W. Zhu, Preparation and properties of barium titanate glass-ceramics sintered from sol–gel-derived powders, Journal of Materials Science. 32 (1997) 3659–3665.
[5] T. KOKUBO, C. KUNG, M. TASHIRO, 14. Preparation of Thin Films of BaTiO3 Glass Ceramics and Their Dielectric Properties, (1968).
[6] S. Hanjitsuwan, P. Chindaprasirt, K. Pimraksa, Electrical conductivity and dielectric property of fly ash geopolymer pastes, International Journal of Minerals, Metallurgy, and Materials. 18 (2011) 94–99.
[7] S. Liu, B. Shen, H. Hao, J. Zhai, Glass–ceramic dielectric materials with high energy density and ultra-fast discharge speed for high power energy storage applications, J. Mater. Chem. C. 7 (2019) 15118–15135. https://doi.org/10.1039/C9TC05253D.
[8] A.K. Yadav, C. Gautam, Dielectric behavior of perovskite glass ceramics, J Mater Sci: Mater Electron. 25 (2014) 5165–5187. https://doi.org/10.1007/s10854-014-2311-6.
[9] Q. Meng, D.D.L. Chung, Battery in the form of a cement-matrix composite, Cement and Concrete Composites. 32 (2010) 829–839. https://doi.org/10.1016/j.cemconcomp.2010.08.009.
[10] J. Zhang, J. Xu, D. Zhang, A Structural Supercapacitor Based on Graphene and Hardened Cement Paste, J. Electrochem. Soc. 163 (2016) E83–E87. https://doi.org/10.1149/2.0801603jes.
[11] A.B. Malkawi, H. Al-Mattarneh, B.E. Achara, B.S. Mohammed, M.F. Nuruddin, Dielectric properties for characterization of fly ash-based geopolymer binders, Construction and Building Materials. 189 (2018) 19–32. https://doi.org/10.1016/j.conbuildmat.2018.08.180.
[12] J. Davidovits, years of successes and failures in geopolymer applications. Market trends and potential breakthroughs, in: Geopolymer Institute Saint-Quentin, France; Melbourne, Australia, 2002: p. 29.
[13] C. Lamuta, S. Candamano, F. Crea, L. Pagnotta, Direct piezoelectric effect in geopolymeric mortars, Materials & Design. 107 (2016) 57–64.
[14] S. Hanjitsuwan, S. Hunpratub, P. Thongbai, S. Maensiri, V. Sata, P. Chindaprasirt, Effects of NaOH concentrations on physical and electrical properties of high calcium fly ash geopolymer paste, Cement and Concrete Composites. 45 (2014) 9–14. https://doi.org/10.1016/j.cemconcomp.2013.09.012.
[15] J. Davidovits, Geopolymers, Journal of Thermal Analysis and Calorimetry. 37 (1991) 1633–1656. https://doi.org/10.1007/BF01912193.
[16] M. Saafi, A. Gullane, B. Huang, H. Sadeghi, J. Ye, F. Sadeghi, Inherently multifunctional geopolymeric cementitious composite as electrical energy storage and self-sensing structural material, Composite Structures. 201 (2018) 766–778. https://doi.org/10.1016/j.compstruct.2018.06.101.
[17] M. Rowles, B. O'connor, Chemical optimisation of the compressive strength of aluminosilicate geopolymers synthesised by sodium silicate activation of metakaolinite, Journal of Materials Chemistry. 13 (2003) 1161–1165.
[18] N. Hu, D. Bernsmeier, G.H. Grathoff, L.N. Warr, The influence of alkali activator type, curing temperature and gibbsite on the geopolymerization of an interstratified illite-smectite rich clay from Friedland, Applied Clay Science. 135 (2017) 386–393. https://doi.org/10.1016/j.clay.2016.10.021.

[19] S.A. Bernal, R.S. Nicolas, J.S.J. van Deventer, J.L. Provis, Alkali-activated slag cements produced with a blended sodium carbonate/sodium silicate activator, Advances in Cement Research. 28 (2015) 262–273. https://doi.org/10.1680/jadcr.15.00013.
[20] A. Fernández-Jiménez, F. Puertas, Setting of alkali-activated slag cement. Influence of activator nature, Advances in Cement Research. 13 (2001) 115–121. https://doi.org/10.1680/adcr.2001.13.3.115.
[21] T.W. Dakin, Conduction and polarization mechanisms and trends in dielectric, IEEE Electrical Insulation Magazine. 22 (2006) 11–28. https://doi.org/10.1109/MEI.2006.1705854.
[22] G. Goracci, M. Monasterio, H. Jansson, S. Cerveny, Dynamics of nano-confined water in Portland cement-Comparison with synthetic CSH gel and other silicate materials, Scientific Reports. 7 (2017) 1–10.
[23] S.M. Rhim, S. Hong, H. Bak, O.K. Kim, Effects of B2O3 addition on the dielectric and ferroelectric properties of Ba0. 7Sr0. 3TiO3 ceramics, Journal of the American Ceramic Society. 83 (2000) 1145–1148.
[24] Z. Jiwei, Y. Xi, C. Xiaogang, Z. Liangying, H. Chen, Direct-current field dependence of dielectric properties in B2O3-SiO2 glass doped Ba0. 6Sr0. 4TiO3 ceramics, Journal of Materials Science. 37 (2002) 3739–3745.
[25] Q. Zhang, J. Cui, G. Dong, J. Du, The effect of lead-glass additives on densification and dielectric properties of Ba0. 4Sr0. 6TiO3 ceramics, in: IOP Publishing, 2009: p. 012066.
[26] X.-M. Cui, G.-J. Zheng, Y.-C. Han, F. Su, J. Zhou, A study on electrical conductivity of chemosynthetic Al2O3–2SiO2 geoploymer materials, Journal of Power Sources. 184 (2008) 652–656. https://doi.org/10.1016/j.jpowsour.2008.03.021.
[27] X. Cui, L. Liu, Y. He, J. Chen, J. Zhou, A novel aluminosilicate geopolymer material with low dielectric loss, Materials Chemistry and Physics. 130 (2011) 1–4. https://doi.org/10.1016/j.matchemphys.2011.06.039.
[28] A. Deschanvres, B. Raveau, F. Tollemer, Substitution of copper for a divalent metal in perovskite-type titanates, Bull. Soc. Chim. Fr. 11 (1967) 4077–4078.
[29] U.S. Rai, L. Singh, K.D. Mandal, N.B. Singh, An Overview on Recent Developments in the Synthesis, Characterization and Properties of High Dielectric Constant Calcium Copper Titanate Nano-Particles, (2014) 18.
[30] J. Shankar, V. Deshpande, Electrical and thermal properties of lead titanate glass ceramics, Physica B: Condensed Matter. 406 (2011) 588–592.
[31] C. Acar, A comprehensive evaluation of energy storage options for better sustainability, International Journal of Energy Research. 42 (2018) 3732–3746. https://doi.org/10.1002/er.4102.
[32] X. He, Y. Zhu, Y. Mo, Origin of fast ion diffusion in super-ionic conductors, Nat Commun. 8 (2017) 15893. https://doi.org/10.1038/ncomms15893.
[33] R. Bulatova, M. Jabbari, A. Kaiser, M. Della Negra, K.B. Andersen, J. Gurauskis, C.R.H. Bahl, Thickness control and interface quality as functions of slurry formulation and casting speed in side-by-side tape casting, Journal of the European Ceramic Society. 34 (2014) 4285–4295. https://doi.org/10.1016/j.jeurceramsoc.2014.07.013.
[34] A.I.Y. Tok, F.Y.C. Boey, Y.C. Lam, Non-Newtonian fluid flow model for ceramic tape casting, Materials Science and Engineering: A. 280 (2000) 282–288. https://doi.org/10.1016/S0921-5093(99)00691-7.

[35] R.J. Nava Quintero, S. Guillemet, J.A. Aguilar-Garib, M.E. Reyes Melo, B. Durand, The thickness of BaTiO3 tape castings as function of the slip system, Journal of Ceramic Processing Research. 13 (2012) 101–104.
[36] Q. Tang, Y. Ge, K. Wang, Y. He, X. Cui, Preparation and characterization of porous metakaolin-based inorganic polymer spheres as an adsorbent, Materials & Design. 88 (2015) 1244–1249. https://doi.org/10.1016/j.matdes.2015.09.126.
[37] K. Aoki, K. Kusakabe, S. Morooka, Separation of Gases with an A-Type Zeolite Membrane, Ind. Eng. Chem. Res. 39 (2000) 2245–2251. https://doi.org/10.1021/ie990902c.
[38] I. Kiesow, D. Marczewski, L. Reinhardt, M. Mühlmann, M. Possiwan, W.A. Goedel, Bicontinuous Zeolite Polymer Composite Membranes Prepared via Float Casting, J. Am. Chem. Soc. 135 (2013) 4380–4388. https://doi.org/10.1021/ja311785f.